

# Numerical solution of the 2D transient heat conduction equation

Derek W. Harrison

October 6, 2020

## Introduction

The 2D transient heat conduction equation is solved numerically using the finite volume method. Central differencing is applied to the diffusion terms and time discretization is fully implicit. The resulting linear system is solved using the incomplete Cholesky factorization conjugate gradient method (ICCG).

## Model equations

From an energy balance at an arbitrary location in the domain  $V$  it follows that the equation for transient heat conduction is given by:

$$\rho C_p \frac{\partial T}{\partial t} = \lambda \nabla^2 T + q \quad (1)$$

With  $\rho$  the density,  $C_p$  the heat capacity,  $T$  the temperature,  $\lambda$  the heat conduction coefficient and  $q$  the source term. The source term  $q$  can be a function of the domain coordinates and time. The temperature  $f$  is specified at the boundaries  $\partial V$ :

$$T(\mathbf{x}) = f(\mathbf{x}) \quad \forall x, y \in \partial V \quad (2)$$

With  $\mathbf{x}$  the position vector and  $x$  and  $y$  the coordinates.

## ICCG algorithm

The ICCG algorithm computes the solution to the linear system:

$$M\mathbf{x} = \mathbf{y} \quad (3)$$

Where  $M$  is symmetric and positive definite and is the linear system obtained from discretization of the transient heat conduction equation,  $\mathbf{x}$  is the temperature distribution to be computed and  $\mathbf{y}$  is the set of source terms of the discretized equations.

Before the algorithm is executed, incomplete Cholesky factorization is applied to  $M$  resulting in a lower triangular matrix  $L$  with the same sparsity as  $M$  and an initial estimate  $\mathbf{x}_0$  of the temperature distribution is made. Then, the initial residuals  $\mathbf{r}_0 = \mathbf{y} - M\mathbf{x}_0$  and the quantity  $\mathbf{p}_0 = (LL^T)^{-1}\mathbf{r}_0$  are calculated. Now, the required initial quantities have been calculated and the algorithm can be executed.

The algorithm consists of the following steps [1]:

$$\alpha_i = (\mathbf{r}_i \cdot (LL^T)^{-1}\mathbf{r}_i) / (\mathbf{p}_i \cdot M\mathbf{p}_i) \quad (4)$$

$$\mathbf{x}_{i+1} = \mathbf{x}_i + \alpha_i \mathbf{p}_i \quad (5)$$

$$\mathbf{r}_{i+1} = \mathbf{r}_i - \alpha_i M\mathbf{p}_i \quad (6)$$

$$\beta_i = (\mathbf{r}_{i+1} \cdot (LL^T)^{-1}\mathbf{r}_{i+1}) / (\mathbf{r}_i \cdot (LL^T)^{-1}\mathbf{r}_i) \quad (7)$$

$$\mathbf{p}_{i+1} = (LL^T)^{-1}\mathbf{r}_{i+1} + \beta_i \mathbf{p}_i \quad (8)$$

Steps (4) to (8) are repeated until the error  $|\mathbf{r}|$  is below some threshold  $\epsilon$ .

## Verification

To verify the algorithm is working properly some cases are considered for which analytical solutions can be obtained. These are then compared with the results obtained from simulation.

### Steady state solutions

For long exposure times the system achieves thermal equilibrium. Several of such cases, for which analytical solutions can be obtained, are examined.

#### Case 1

The first case used for verification is:

$$\nabla^2 T - \sin(\pi x) \sin(\pi y) = 0 \quad (9)$$

With boundary conditions:

$$T = 0 \quad \forall x, y \in \partial V \quad (10)$$

The coordinates  $x$  and  $y$  range from 0 to 1. Equation (9) has the following analytical solution:

$$T = -\frac{\sin(\pi x) \sin(\pi y)}{2\pi^2} \quad (11)$$

Comparison of numerical results, obtained with a grid resolution of 40 nodes along each axis, with the analytical solution shows that the difference between numerical and analytical solutions is 0.05 %. A visualization of the results is given in figures 1 and 2.

#### Case 2

The second case used for verification is:

$$\nabla^2 T - q = 0 \quad (12)$$

With boundary conditions:

$$T = 0 \quad \forall x, y \in \partial V \quad (13)$$

The coordinates  $x$  and  $y$  range from 0 to 1. Equation (12) has the following analytical solution:

$$T = \frac{q}{2\lambda}(w^2 - x^2) - 16w^2 \frac{q}{\lambda\pi^3} \sum_{n=0}^{\infty} \frac{(-1)^n}{(2n+1)^3} \frac{\cos((2n+1)\frac{\pi x}{2w}) \cosh((2n+1)\frac{\pi y}{2w})}{\cosh((2n+1)\frac{\pi h}{2w})} \quad (14)$$

Where  $w = L_x/2$  and  $h = L_y/2$  with  $L_x$  the length of the domain along the  $x$  coordinate and  $L_y$  the length of the domain along the  $y$  coordinate. The  $x$  and

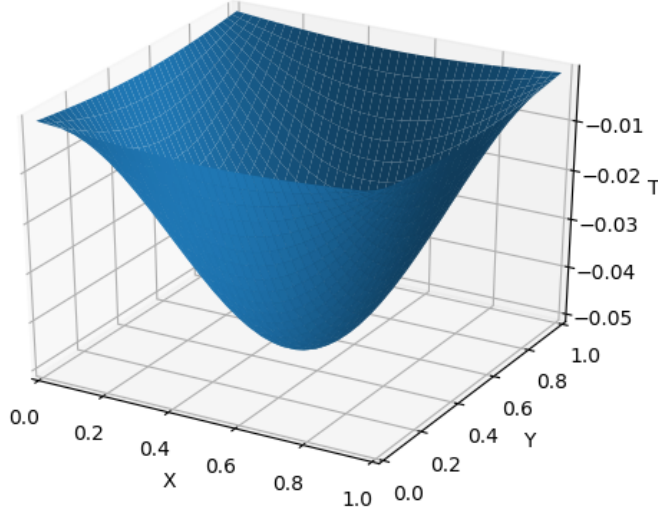


Figure 1: Numerical results case 1

$y$  coordinates in equation (14) specify the position relative to the origin  $(0,0)$ . The numerical solution however, places the origin at  $(0.5,0.5)$ . In order to compare analytical with numerical results the results obtained from the analytical solution must be shifted.

Comparison of numerical results, obtained with a grid resolution of 40 nodes along each axis, with the analytical solution shows that the difference between numerical and analytical solutions is 0.51 %. A visualization of the results is given in figures 3 and 4.

### Case 3

The third case used for verification is:

$$\nabla^2 T = 0 \quad (15)$$

With boundary conditions:

$$T = 0 \quad \forall x, y \in \partial V \quad (16)$$

Except when  $y = L_y$ , where the temperature is equal to 100, i.e.: the northern boundary temperature is 100. The  $x$  coordinates range from 0 to 0.1 and the

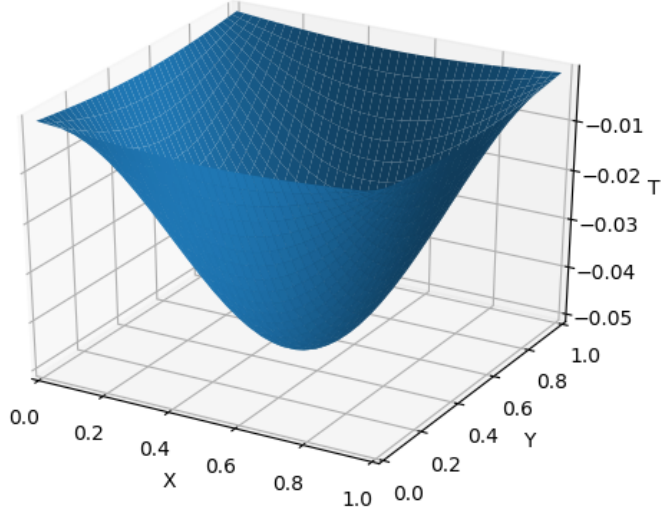


Figure 2: Analytical results case 1

$y$  coordinates range from 0 to 0.15. Equation (15) with the given boundary conditions has the following analytical solution:

$$T = \frac{400}{\pi} \sum_{n=1,3}^{\infty} \frac{\sinh(n\pi y/L_x) \sin(n\pi x/L_x)}{n \sinh(n\pi L_y/L_x)} \quad (17)$$

Comparison of numerical results, obtained with a grid resolution of 80 by 120 nodes, with the analytical solution shows that the difference between numerical and analytical solutions is 0.05 %. A visualization of the results is given in figures 5 and 6.

#### Case 4

The fourth case used for verification is:

$$\nabla^2 T + 5\pi^2 \sin \pi x \cos 2\pi y = 0 \quad (18)$$

With boundary conditions:

$$T(x, 0) = \sin \pi x \quad (19)$$

$$T(x, 1) = \sin \pi x \quad (20)$$

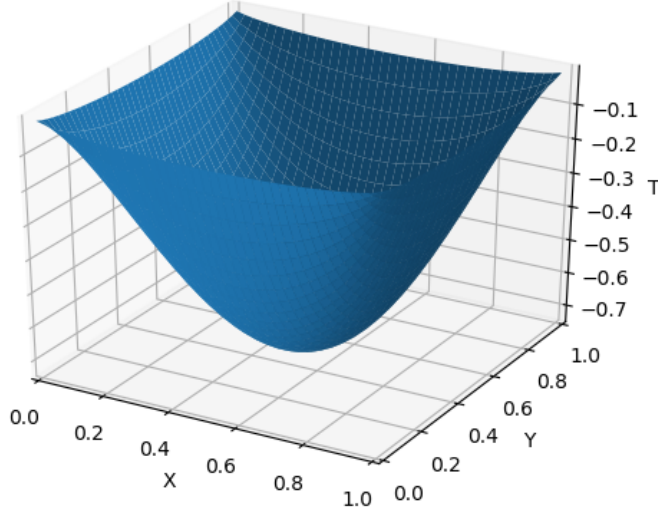


Figure 3: Numerical results case 2

The remaining boundaries are set to 0. The coordinates  $x$  and  $y$  range from 0 to 1. Equation (18) has as analytical solution:

$$T = \sin(\pi x) \cos(2\pi y) \quad (21)$$

Comparison of numerical results, obtained with a grid resolution of 40 nodes along each axis, with the analytical solution shows that the difference between numerical and analytical solutions is 0.28 %. A visualization of the results is given in figures 7 and 8.

### Case 5

The fifth case used for verification is:

$$\nabla^2 T - 6xy(1 - y) + 2x^3 = 0 \quad (22)$$

With boundary conditions:

$$T(1, y) = y(1 - y) \quad (23)$$

The remaining boundaries are set to 0. The coordinates  $x$  and  $y$  range from 0 to 1. Equation (22) with the given boundary conditions has as analytical solution:

$$T = y(1 - y)x^3 \quad (24)$$

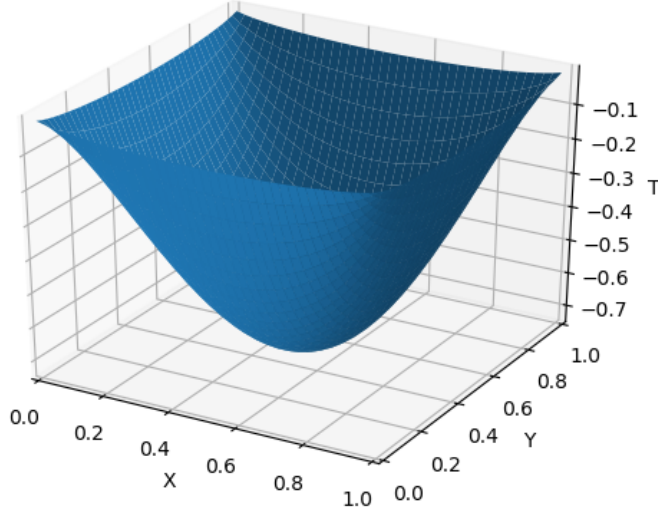


Figure 4: Analytical results case 2

Comparison of numerical results, obtained with a grid resolution of 40 nodes along each axis, with the analytical solution shows that the difference between numerical and analytical solutions is 0.68 %. A visualization of the results is given in figures 9 and 10.

### Short exposure times

For short exposure times, such that the temperature at the center of the material does not change appreciably (i.e.: for small Fourier numbers  $Fo = \alpha t/d^2 < 0.1$ ), penetration theory can be applied to determine the flux  $g$  at the boundary:

$$g = \lambda \frac{T_1 - T_0}{\sqrt{\pi \alpha t}} \quad (25)$$

Where  $T_1$  is the temperature at the boundaries,  $T_0$  is the initial temperature,  $\alpha$  the thermal diffusivity and  $t$  time. Setting the boundary temperature  $T_1$  to 1, the initial temperature  $T_0$  to 0, the heat conduction coefficient to 1 and the thermal diffusivity to 1 gives the following relation for the flux:

$$g = \frac{1}{\sqrt{\pi t}} \quad (26)$$

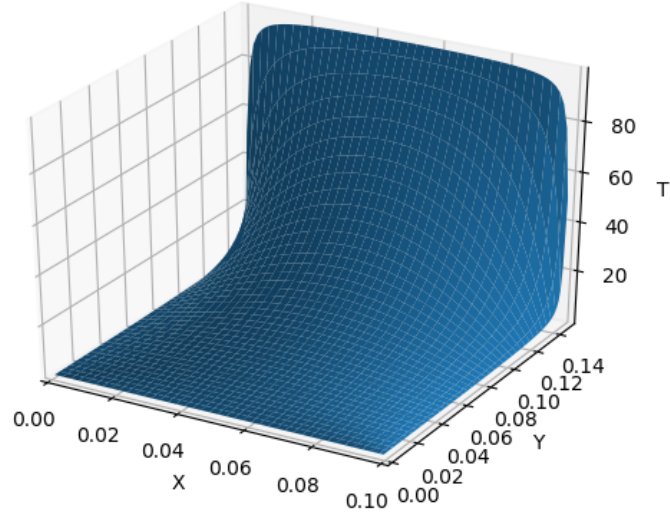


Figure 5: Numerical results case 3

Equation (26) is compared with the flux computed numerically using a system with a grid resolution of 40 nodes along each axis and grid coordinates  $x$  and  $y$  ranging from 0 to 1. Results are shown in table 1.

Table 1: Numerical and analytical flux data.

$t$	Flux analytical	Flux numerical
0.0001	56.42	61.81
0.0002	39.89	41.46
0.0003	32.57	33.37
0.0004	28.21	28.73
0.0005	25.23	25.60
0.0075	20.60	20.81
0.001	17.84	17.98
0.002	12.62	12.67
0.003	10.30	10.34



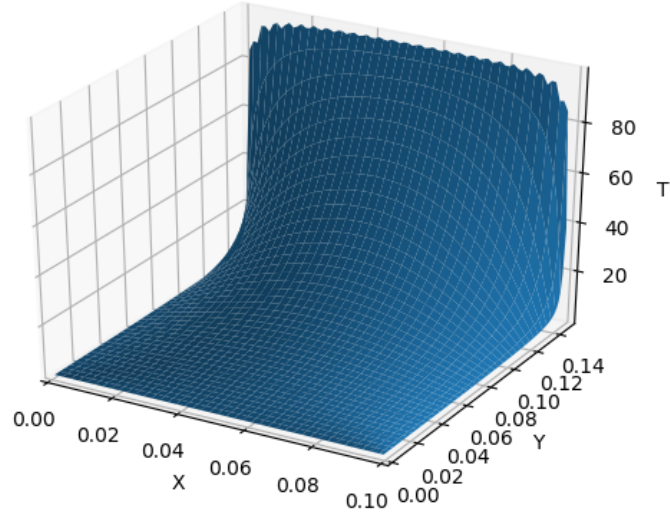


Figure 6: Analytical results case 3

### Moderate exposure times

For moderate exposure times, such that  $Fo = \alpha t/d^2 > 0.1$ , the temperature distributions  $M = (T_1 - T_c)/(T_1 - T_0)$  obtained from simulations are compared with data tabulated in [2], where  $T_1$  is the temperature of the boundary,  $T_c$  the temperature at the center and  $T_0$  is the initial temperature distribution.

Table 2: Temperature distribution data.

$Fo$	M tabulated	M simulation
0.05	0.63	0.60
0.1	0.24	0.23
0.15	0.089	0.085
0.2	0.031	0.032
0.25	0.012	0.012
0.3	0.0043	0.0045
0.35	0.0017	0.0017

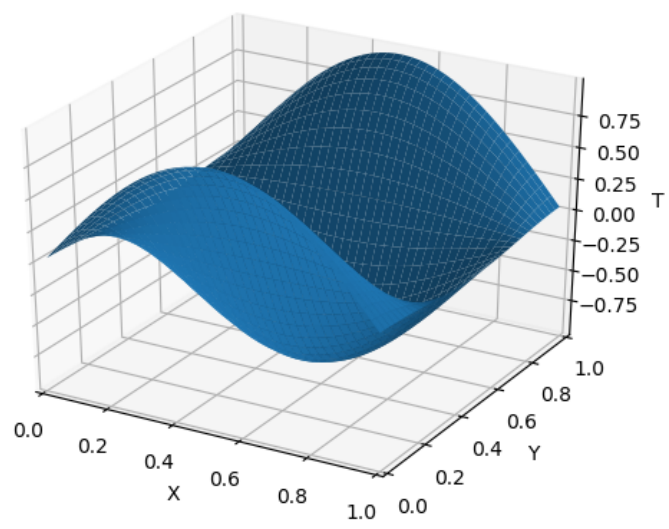


Figure 7: Numerical results case 4

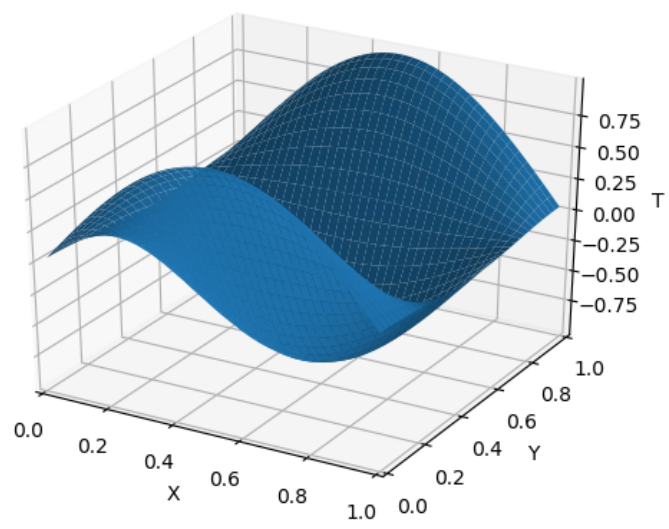


Figure 8: Analytical results case 4

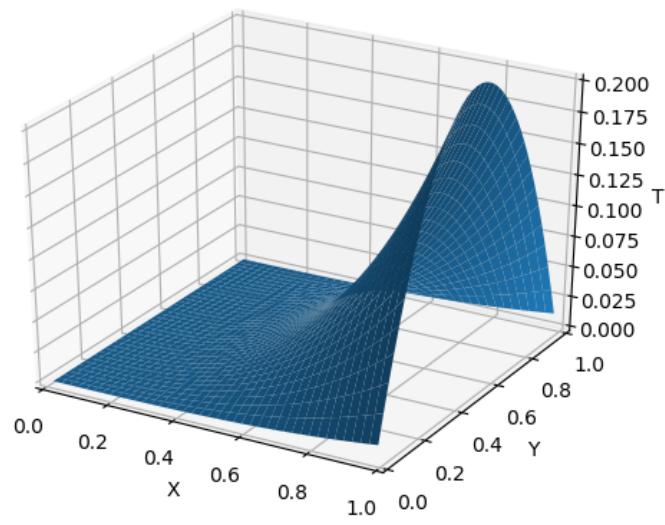


Figure 9: Numerical results case 5

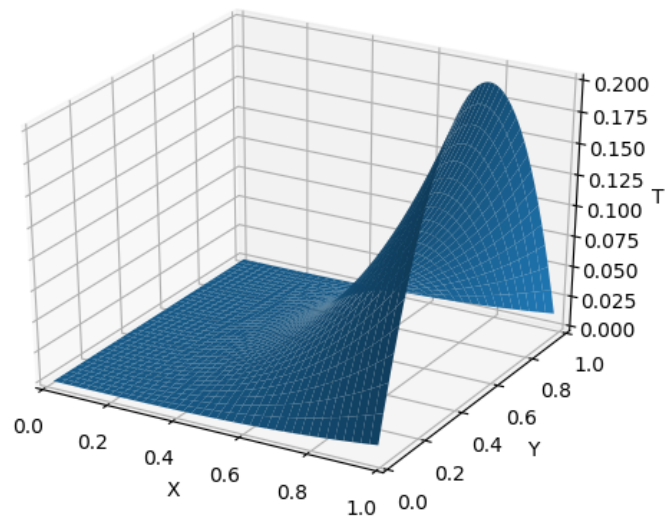


Figure 10: Analytical results case 5

# References

- [1] David S. Kershaw. The incomplete Cholesky-conjugate gradient method for the iterative solution of systems of linear equations. *J. Comp. Phys.* 26, 43-65, 1978.
- [2] L.P.B.M Janssen and M.M.C.G Warmoeskerken. Transport phenomena data companion. 2006.